

Studies on the energy and deep memory behaviour of a cache-oblivious, task-based hyperbolic PDE solver

Dominic E. Charrier

Durham University
Stockton Road

Durham DH1 3LE, Great Britain
dominic.e.charrier@durham.ac.uk

Benjamin Hazelwood

Durham University
Stockton Road

Durham DH1 3LE, Great Britain
benjamin.hazelwood@durham.ac.uk

Andrey Kudryavtsev

Intel
1900 Prairie City Rd
Folsom, California, United States
andrey.o.kudryavtsev@intel.com

Alexander Moskovsky

RSC Group
Kutuzovskiy av., 36
Moscow 121170, Russia
moskov@rsc-tech.ru

Ekaterina Tutlyaeva

RSC Group
Kutuzovskiy av., 36
Moscow 121170, Russia
xgl@rsc-tech.ru

Tobias Weinzierl

Durham University
Stockton Road
Durham DH1 3LE, Great Britain
tobias.weinzierl@durham.ac.uk

ABSTRACT

We study the behaviour of a seismic simulation on a server with an Intel® Optane™ memory subsystem. The simulation uses the ExaHyPE engine. ExaHyPE combines dynamically adaptive meshes (AMR) with ADER-DG. It is parallelised using tasks, and it is cache efficient. AMR plus ADER-DG yields a task graph which is highly dynamic in nature and comprises both arithmetically expensive and bandwidth-intense tasks. Despite this inhomogeneous character, our code benefits from AVX vectorization, though it suffers from memory access bursts. We show that a frequency reduction of the chip does not mitigate burst effects although it improves the code’s energy-to-solution. Even worse, the burst’s latency dependence becomes worse once we add Optane. However, in cases where memory-intense and computationally expensive tasks overlap, ExaHype’s cache-oblivious implementation can exploit the Intel Memory Drive Technology (IMDT) virtualizing the extra memory layer, and it suffers only from a less than 3× performance decline per degree of freedom versus pure DDR4 memory. We thus propose that upcoming supercomputing simulation codes with dynamic, inhomogeneous task graphs require algorithms and task schedulers which actively prefetch data, intermix tasks of different character, and apply frequency control to or switch off the memory if appropriate.

ACM Reference format:

Dominic E. Charrier, Benjamin Hazelwood, Andrey Kudryavtsev, Alexander Moskovsky, Ekaterina Tutlyaeva, and Tobias Weinzierl. 2016. Studies on the energy and deep memory behaviour of a cache-oblivious, task-based hyperbolic PDE solver. In *Proceedings of ACM Conference, Washington, DC, USA, July 2017 (Conference’17)*, 9 pages.

DOI: 10.1145/nnnnnnnnnnnnnnnn

Permission to make digital or hard copies of all or part of this work for personal or classroom use is granted without fee provided that copies are not made or distributed for profit or commercial advantage and that copies bear this notice and the full citation on the first page. Copyrights for components of this work owned by others than ACM must be honored. Abstracting with credit is permitted. To copy otherwise, or republish, to post on servers or to redistribute to lists, requires prior specific permission and/or a fee. Request permissions from permissions@acm.org.

Conference’17, Washington, DC, USA

© 2016 ACM. 978-x-xxxx-xxxx-x/YY/MM...\$15.00

DOI: 10.1145/nnnnnnnnnnnnnnnn

1 INTRODUCTION

The memory architectures in mainstream supercomputing (Intel-inspired architectures) become more and more inhomogeneous and flexible. We classify these trends into clocktick—modern architectures can modify the chip frequencies of some components—vertical and horizontal inhomogeneity. Modern memory hierarchies are built in layers with the chip’s registers on the top and the persistent memory at the bottom. This yields a vertical dimension. Horizontally, two-socket systems dominate the market. Though the main memory and some intermediate memory layers are logically shared between all cores, the chip technically is split up into sets of cores with their own memories and memory controllers. Data access cost within one layer depend on whether data resides on the local segment of memory or has to be fetched from memory technically associated to the other set of cores. Access cost are non-uniform (NUMA). Vertically, cached systems dominate the market. As access from the CPU to the main memory is very expensive, intermediate memory layers hold data copies temporarily. Small intermediate memory layers can deliver data quick to the cores. Synchronization mechanisms such as MeSA and its extensions between the temporary memories ensures vertical and horizontal data consistency between caches, cores and main memory.

Neither vertical and horizontal diversity nor frequency alterations are new. Their character however evolves and their impact on code performance increases. There are at least three hardware evolution trends to cause this: With an increase of core counts, NUMA effects gain importance. More cores and their caches have to be synchronised, while the pressure on the main memory increases. With the arrival of more inhomogeneous or new beyond-main memory storage technology (Intel® Optane™ Technology or MCDRAM), we witness either an additional cache layer or increased non-uniformism when it comes to memory accesses. Prefetching, capacity, latency and bandwidth impact change. With the opportunity to down- or upclock system components—either triggered by users or the energy controllers on the board—we finally face further fluctuations in effective speed.

In many HPC application fields, the technological trends are accompanied by changing application characteristics. While they seem to fit more or less seamlessly to codes with structured data,

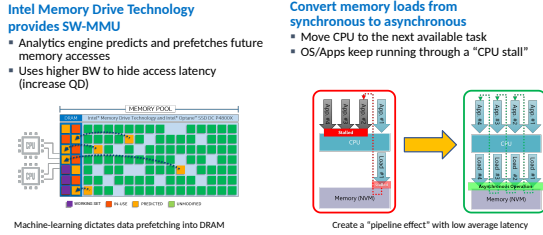


Figure 1: The Intel Memory Drive Technology (IMDT) operation mode for Optane.

homogeneous compute characteristics, invariant memory footprint and regular data access—for such codes, data locality and caching are well understood while any downclocking applies to all code components uniformly—many top notch simulation codes move away from such data access patterns. They work with adaptive mesh refinement (AMR), where memory footprint and access character change all the time, and they employ numerical schemes with multifaceted compute characteristics. Some compute steps are intense w.r.t. memory accesses, some compute-bound.

Many memory hardware trends have not been introduced in a co-design approach with modern HPC codes. They are imposed on HPC simulations by the vendors. New memory layers typically deliver improved bandwidth and storage size, but also increase latency. For embarrassingly parallel codes streaming data through the cores as we find them in machine learning or in-memory database systems [2], this does not pose a problem: threads accessing remote memory are postponed and switched with other threads. We “asynchronize” threads and memory accesses. Intel’s Optane IMDT is explicitly built with this in mind (Fig.1). Such a programming model, being similar to CUDA, does not fit to many modern HPC codes which have not been designed a priori for this purpose. All concurrency is typically already exploited with the given number of cores and cannot be increased arbitrarily. Cache access is optimised w.r.t. data reusage and suffers from context switches. Per thread data access is organised to be continuous and in a streaming fashion to fit to vector compute units, so any interference destroys the vector efficiency. Nevertheless, it is interesting for HPC codes to question whether additional memory layers and complexity help us to simulate bigger setups.

Our case study examines the LOH.1 benchmark, a standard benchmark for earthquake simulations. The underlying wave equations are solved in first-order formulation through ExaHyPE [1] whose mathematical concept is based upon ADER-DG [5]. Its task-based realization simulates wave propagation on dynamically adaptive meshes which are allowed to change in each time step. This implies that (i) very compute-intense steps take turns with tasks that are computationally cheap but process reasonably large amounts of data; (ii) the memory demands change as dynamic mesh refinement aggregates additional blocks in the main memory while mesh coarsening releases memory segments; (iii) the concurrency profile of the code is time-dependent and changing such that dynamic tasking with task stealing is required. ADER-DG yields an application with very irregular and inhomogeneous memory access as well as multifaceted arithmetic intensity patterns at a limited concurrency level. Yet, the code base is carefully designed to be cache-oblivious and memory access modest [4], and it has access

to aggressively vectorised compute kernels for its compute-intense tasks. For the latter, we rely on work by M. Bader and J.-M. Gallard, while the actual LOH.1 implementation is provided by M. Bader, K. Duru, A.-A. Gabriel and L. Rannabauer. Codes alike ExaHyPE with ADER-DG are prime candidates to benefit from dramatically increased per-node memory. First, high-order approaches are one way forward to exploit vectorization. However, using very high order approaches implies that the number of mesh elements per node is typically comparably low. If the mesh element cardinality determines the concurrency levels, we face limited strong scaling potential. The only solution is to increase both the polynomial order and the mesh sizes. Second, interconnect infrastructure is expensive and often a bottleneck. Larger memory allows us to upscale the per-node problem sizes and, thus, to diminish latency and bandwidth penalties, if the computational workload can be upscaled relative to the communication demands. Third, explicit time stepping codes suffer from small admissible time step sizes on the extreme scale through the CFL condition. One way to resolve this is to switch to (locally) implicit approaches of high order in time; such as ADER-DG. This amplifies all memory demands. In no case should upscaling the per-node problem size come at the cost of a significant per-node performance degradation permitted by new memory or dramatically increase hunger for energy.

By means of our non-trivial benchmark setup and reasonable core-per-node counts, we follow up on two research questions:

- What role do frequency changes play in terms of time-of-solution and energy-of-solution? Which impact does AVX with its downclocking have on the energy efficiency and time-to-solution?
- How do additional memory layers such as Optane affect the algorithm if the main memory is transformed into a cache? Can techniques such as core oversubscription be used?

Our data clarify that there is a frequency sweet spot w.r.t. the most efficient energy usage vs. runtime. It is significantly below the peak performance frequency. However, the impact of frequency reductions diminishes if we use additional memory levels, as the power consumption of Optane remains roughly constant for our benchmarks. From a performance point of view, oversubscribing cores to mitigate latency effects from additional memory is counterproductive. We show that it is absolutely essential to equip tasking systems and algorithms with the opportunity to run memory-intense and compute-bound tasks concurrently, while the majority of compute-intense jobs has to exhibit data access locality. If we get the balance between bandwidth and compute demands right, latency effects remain under control. The access pattern has to be homogenised. To the best of our knowledge, this is the first study with such a complex HPC algorithm that uses Optane, it contributes novel insight on the energy impact of the memory, and it is the first explicit clarification on the importance of memory access homogenization for Optane.

The case study is structured as follows: We give an overview over our benchmark code base ExaHyPE in Section 2, before we describe the two test machines. In Section 4, we present our benchmark data, which allows us to reason about algorithmic implications on massively parallel task systems in the conclusion (Section 5).

2 THE EXAHYPE BENCHMARK CODE

Our experiments study the LOH.1 benchmark (cf. [5]) which is realized through the ExaHyPE engine [1]. LOH.1 is an artificial seismic earthquake scenario benchmark. A cubic domain is split up into two horizontal layers of material, and an earthquake is induced as point source inside the cube. Sensors close to the domain surface track incoming waves. A feature-based refinement criterion follows the steepest solution gradients and shocks. The mesh spreads from the point source. While LOH.1 is an artificial, idealised setup, it exhibits real-world simulation characteristics with its material transition, a source term and non-trivial inference and reflection patterns.

ExaHyPE solves hyperbolic differential equations of first order with ADER-DG. ADER-DG is a predictor-corrector scheme [5] which traverses a grid tessellating the computational domain and first computes per mesh cell a predicted solution evolution. This prediction is of the same order in time as the spatial order (typically $p \in \{3, 4, \dots, 9\}$) and is determined implicitly. Solving such an implicit space-time problem is computationally possible as we neglect the solution in neighbouring cells. It is a cell-local prediction. The implicit solve of high order renders the predictor computationally intense. Riemann solves in a second step tackle the arising jumps in the predicted solutions along cell faces, before a corrector step sums up the result of the prediction and the Riemann solves. These two follow-up steps are arithmetically cheap. Measurements show that they require more bandwidth [4]. We consider ADER-DG interesting from a forward-looking HPC point of view, as arithmetically intense steps take turns with memory movement-intense steps per time step. We do not have a homogeneous compute profile.

ExaHyPE employs a dynamically adaptive Cartesian grid. It is constructed from a spacetree [13, 14]. The term spacetree describes a generalization of the octree/quadtree concept. The meshing supports dynamically adaptive grids which may change in each and every time step. On purpose, we thus neglect multi-node runs. They inevitably yield load balancing challenges which hide the per-node memory effects studied here. The mesh topology determines which ADER-DG tasks can be run in parallel [3]: For example, all Riemann solves are embarrassingly parallel but require input from their two neighbouring cells. Along adaptivity boundaries, more than two cells are involved. As the adaptivity changes, every time step induces a different multicore task pattern, i.e. the sequence and structure of parallel work items never is the same between any two time steps. We do not have a invariant task graph.

For Intel-based architectures, ExaHyPE offers tailored compute kernels. As soon as architecture, number of equation unknowns, PDE term types and polynomial orders are known—as they are for our LOH.1 setup—ExaHyPE’s compute ecosystem can rewrite the most time-consuming code parts into highly efficient, vectorized, tailored code kernels. For these, it employs AVX instructions, appropriate alignment and padding, aggressive function inlining, as well as rephrasing of code parts into small matrix-vector products [8]. Experiments with loop-based parallelism within these kernels clarified that loop-based parallelization of the compute kernels did not yield further speedup on top of the task-based parallelism.

2.1 Homogenization of the task execution

In ADER-DG, all cell-based (correction and prediction) tasks are independent of each other cells. All Riemann tasks are independent of each other, too. Between those types, dependencies exist: A predictor requires the input from the correction which in turn requires the result of 2d Riemann solves. Each Riemann solve requires input from the two predictions of adjacent cells.

ExaHyPE offers two task processing modi. In its basic variant, it first issues one type of task, processes these tasks (which are all independent of each other), and then continues with the next type of tasks. It yields one (predictor) sweep with very high arithmetic intensity, followed by a sweep which is not compute-intense. Dynamic adaptivity introduces additional memory-intense steps preluding the invocation of computationally heavy tasks. Each sweep is homogeneous w.r.t. its compute profile. The total time step however exhibits inhomogeneous character. This scheme is equivalent to a breadth-first traversal of the task graph.

An alternative variant is the fused mode [4]. It issues a task as soon as its input data are available. A Riemann solve starts as soon as the predictions of the two adjacent cells become available—it does not wait for all predictions to terminate—and a corrector task is issued immediately once all 2d Riemann solves on the cell’s adjacent faces are solved. We issue tasks as soon as possible even, if this requires some overhead to find out whether a task is already ready.

The latter approach allows for an orchestration of compute-intense parallel to bandwidth-intense tasks. This homogenizes, i.e. averages the character of the tasks over a time step. Furthermore, it increases data access locality. Data are immediately reused: once a computation with a piece of data unlocks the follow-up task (on these data), this follow-up tasks is issued by the fused compute mode. Though we have no absolute control on the processing order of the tasks—this is up to the task runtime—we may assume that the task graph is processed close to a depth-first order.

2.2 Temporal and spatial blocking

ADER-DG’s predictor implicitly realizes spatial and temporal blocking of data accesses [9]: The expensive implicit solves are not ran on the whole mesh but on a per-cell basis. This means many floating point operations are executed over a relatively small set of data. On top of this, ExaHyPE’s grid traversal localizes all data accesses further. It traverses the grid along a space-filling curve whose Hölder continuity yields a spatial and temporal locality of data accesses [13]. If the result of a Riemann solve feeds into once adjacent cell, the probability that the second adjacent cell is processed shortly after is high. Together with the optimization resulting from the homogenization, ExaHyPE realizes a cache-oblivious algorithm.

3 BENCHMARK SYSTEM

Our benchmarks are run on two different server configurations. The first one is an Intel Xeon E5-2650V4 (Broadwell) cluster in a two socket configuration with 24 cores. The run at 2.4 GHz. TurboBoost increases this to up to 2.8 GHz, but a core executing AVX(2) instructions might fall back to a minimum of 1.8 GHz to stay within the TDP limits [10]. Each node has access to 64 GB of 2,400 MHz TruDDR4 memory.

Table 1: Speedup of fused mode with homogenised task character against a plain implementation with three steps each processing one set of independent tasks. Results for orders $p \in \{3, 5, 7\}$ for a regular and dynamically adaptive mesh with one additional level of refinement compared to its regular counterpart.

Cores	Regular			Dyn. Adaptive		
	$p = 3$	$p = 5$	$p = 7$	$p = 3$	$p = 5$	$p = 7$
1	1.09	1.04	1.01	1.16	1.06	1.01
12	1.59	1.25	1.06	1.44	1.54	1.18
24	1.65	1.14	1.30	1.40	1.41	1.60

The second one is a dual-socket Intel Scalable Gold 6154 with 36 physical cores, clocked at 3.00 GHz, and equipped with 192 GB of 2,666 MHz DDR4 memory (12 ranks of 16 GB modules). The chip may reduce the base clock frequency to 2.6 GHz for AVX2 and to 2.1 GHz for AVX-512 [15]. To enable high-volume data experiments, a PCI Express non-blocking switch—an original component of RSC hyperconverged platform [7]—was used. For energy efficiency and compactness, the RSC server(s) are liquid cooled.

In our experiments, the latter system is expanded with 6× Intel DC Optane SSD P4800X, i.e. 375 GB, non-volatile memory. The Optane SSDs are connected via PCIe-switch IC to the CPU, while the Intel Memory Drive Technology (version 8.6.2535.19) implements software-defined memory (SDM) on-top of the Intel Optane SSDs (cmp. Fig. 1). This Intel Memory Drive Technology (IMDT) uses part of the overall memory capacity from the DRAM for caching, prefetching, and endurance protection, i.e. the drives become transparently available to the operating system as system memory. Though our memory totals to roughly 1.4 TB, we stick to the default IMDT settings recommended by Intel which limits the available Optane memory to 8× the main memory. Larger ratios than 1 : 8 would lead to performance drops according to the vendor.

All shared memory parallelization relies on Intel’s Threading Building Blocks (TBB) [11] while Intel’s 2018 C++ compiler translated all codes. Manual pinning is realized through CPU masks. On the Broadwell system, we use Likwid [12] to read out hardware counters made available through RAPL. On Skylake without the attached Optane memory, we read RAPL directly. On the Optane testbed, we use two energy sensors provided by RSC which are attached to the board directly: one sensor to the main board, and another independent sensor for Optane board.

4 MEASUREMENTS

Scalability. Before we study our code’s memory and energy characteristics, we validate that the code scales reasonably. Given the horizontal and vertical diversity, it would make limited sense to benchmark serial or non-scaling code. All scalability data stems from the Broadwell, but qualitatively the same data was obtained on Skylake and an older Sandy Bridge architecture. Our experiments track the scalability for various orders $p \in \{3, 5, 7\}$. They either simulate on a regular grid, i.e. add 0 levels of adaptivity, or on an adaptive grid with one additional level of the mesh compared to the regular baseline.

We observe that the benchmark code’s non-fused tasking scales reasonably on one socket if the polynomial order is reasonably high (Fig. 2). If we use the second half of cores too, the parallel efficiency deteriorates. Higher orders mitigate this effect, while dynamic adaptivity makes it worse. The scalability overall is limited. Dynamic adaptivity is not for free. We face a classic strong scaling behaviour. Further increases of the mesh resolution n (growing the mesh with $O(n^d)$ for regular grids) or polynomial order (increase in $O(n^p)$) are impossible due to memory limits.

Observation 1. For our application field, it is advantageous from an efficiency point of view to use very high polynomial orders. However, the code then quickly runs into the memory wall.

If we rewrite our code into a fused variant where a task is immediately triggered once its input data becomes available, we obtain better scaling code. The improved scalability becomes particularly obvious for dynamically adaptive meshes. We have a more complicated task invocation scheme (dependency tracking), but we can hide the increased administrative cost behind computations.

Observation 2. It robustly pays off to issue compute tasks as soon as their input data is available and thus to overlap computationally demanding with memory-intense tasks.

This observation is in line with implicit data access blocking as we find it in Intel’s TBB [11] where the task graph/tree is processed depth-first, though a reasoning solely in lines of data reusage skips the additional notion of the computational tasks’ character. Unless stated otherwise, we continue with the fused scheme from hereon.

Observation 3. Our benchmark quickly enters the strong scaling regime.

This observation is typical for many HPC codes working with dynamically adaptive meshes. They can exploit state-of-the-art multicore processors, but they do not exhibit arbitrary concurrency.

Code characteristics. We continue our benchmarking with performance counter measurements and profiling. Each test is done without any vectorization (disabled at compile time) and with full AVX2 vectorization.

We observe a robust speed improvement through vectorization (Table 2). The reduction of the time-to-solution follows an increase of the Mflop rate of around 50%. Yet, the decrease of scalability implies that we cannot fully benefit from the vectorization. Furthermore, the vectorization impact is diminished by the fact that arithmetically intense tasks take turns with bandwidth-intense activities. The latter can not benefit from vectorization. Finally, we know that AVX effectively reduces the chip’s frequencies, which has an additional throttling effect. The obtained peak performance is 4–8% of the theoretical peak performance of 845 GFlop/s which we consider to be an acceptable ratio for a dynamically adaptive mesh which can change in each and every time step.

Observation 4. AVX robustly improves the runtime.

To track the cache usage pattern, we measure per cache the request and the miss rate. Request rate means number of requests divided by number of instructions. Miss rate means number of requests not served by a cache divided by number of instructions. From

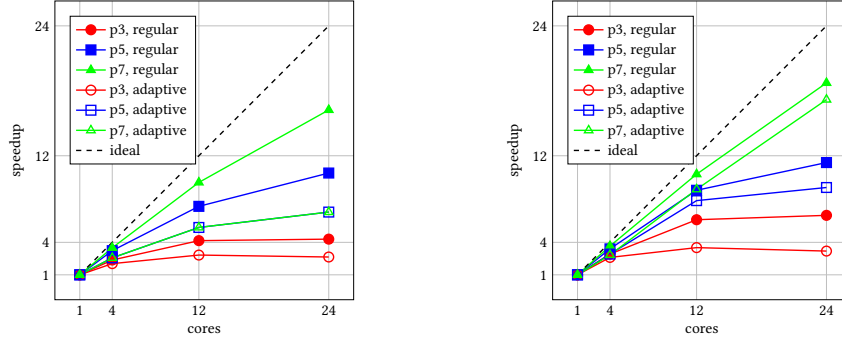


Figure 2: Code scalability on Broadwell for various orders of p and one additional level of dynamically adaptive refinement. We compare a plain realization where we issue first all tasks of the first type, then all of the second type, and so forth (left) with a fused realization where we trigger tasks as soon as possible (right). The regular baseline grid is 27^3 .

Table 2: Hardware counters on Broadwell (24 cores) for a 27^3 grid. Scalar denotes no vectorization (-no-vec).

	Regular						Dyn. Adaptive					
	Scalar			AVX2			Scalar			AVX2		
	$p = 3$	$p = 5$	$p = 7$	$p = 3$	$p = 5$	$p = 7$	$p = 3$	$p = 5$	$p = 7$	$p = 3$	$p = 5$	$p = 7$
Avg. Time (/s)	0.334	0.919	2.16	0.294	0.536	1.34	3.66	5.97	12.0	3.42	4.67	10.2
Gflop/s	11.0	32.4	46.6	14.1	47.9	68.4	2.70	14.7	32.2	4.45	15.5	36.8
L2 Request Rate (%)	5.46	7.64	8.1	9.07	17.82	20.71	4.69	7.01	7.77	7.36	13.11	19.2
L2 Miss Ratio (%)	12.1	14.48	18.74	11.36	14.06	19.26	17.99	14.97	17.57	16.43	15.86	19.13
L3 Request Rate (%)	0.03	0.03	0.04	0.14	0.23	0.29	0.06	0.04	0.04	0.11	0.18	0.22
L3 Miss Ratio (%)	51.2	13.48	9.91	63.5	22.57	12.61	29.39	13.07	6.9	34.77	18.75	9.85
Mem. Bandwidth (GB/s)	10.3	11.0	10.3	17.3	22.2	23.2	4.84	3.56	4.99	6.05	8.99	10.3

both rates, we can derive the miss ratio which is the ratio of cache accesses which have not been served by a particular cache.

The request rate increases with increasing polynomial order. Furthermore, it is significantly higher for AVX-enabled code. While all cache miss rates are negligible, our miss ratio is high: Every time a piece of data is not found in the caches, the next-level cache often cannot serve this request either. This miss ratio decreases with increasing polynomial order. We finally observe that the request rate decreases rapidly over the cache levels. We have not had the opportunity to cross-check our counter data with the Skylake architecture supporting AVX-512 instructions. However, we may assume that the counter behaviour is very similar as all performance measurements are in line with the Broadwell architecture.

Observation 5. Our code is cache efficient on all three levels of caches. However, if a cache request cannot be served, the data likely also are not held in the next level of caches.

Our code works with data in a very localised way. This validates our statements on temporal and spatial blocking within a task-based formalism. Further analysis predicts our code’s compute tasks to yield around 3.5/4.5/4.8 Gflop/s ($p \in \{3, 5, 7\}$) with AVX.

Further benchmarking (Fig. 3) reveals that our code occasionally runs into memory access bursts despite the homogenization used. For the majority of the runtime, the computationally expensive tasks dominate. When all of them are finished, there’s

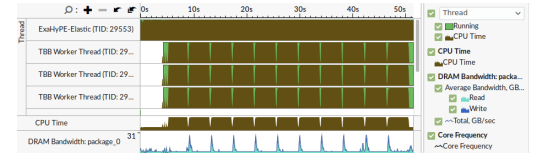


Figure 3: Four-core run with $p = 7$ on a regular grid. We benchmark concurrent computations (brown, top) against memory access (very bottom histogram).

a huge set of memory-intense tasks ready. A significant number of those has to be processed before again a reasonable amount of compute-intense tasks becomes available. Whenever the machine runs out of expensive tasks, bandwidth-intense tasks hammer the memory subsystem. This peak behaviour obviously becomes more significant for the non-homogenised code variant (not shown) where all compute-intense tasks are processed before we issue any bandwidth-intense task. It is also more severe for regular grids. The stronger the adaptivity, the more inhomogeneous the task graph becomes. Memory access bursts disappear behind the computations. The limited scalability plus the mixture with memory-intense jobs plus the extremely dynamic behaviour implies that the code does not perform at a realistic application-peak performance.

While the arithmetically intense prediction jobs access their data continuously, the overall code does not work in a classic streaming way. This is typical for task-based approaches. Two independent

tasks within the ready queue that are processed after each other by one thread rarely share any data or read one data region continuously. Classic stream-oriented, cache-line based prefetching struggles to anticipate this behaviour. As a result, even the bandwidth peaks are not even close to the machine’s maximum throughput, for which the Stream TRIAD benchmark specifies 112 GByte/s.

Our code is never bandwidth-bound, but it is latency sensitive. Due to the very good localization of all data access, we do not exploit the available memory bandwidth on the test machine on any cache level. AVX increases the bandwidth requirements—more data is to be piped through the hierarchy—as the required additional padding and alignment increases the memory footprint. Yet, these increases do not move the bandwidth requirements anywhere near to the maximum bandwidth, and they do not lead to a higher cache miss ratio. As a consequence, an increase of bandwidth between the caches is of limited use to our code base:

Observation 6. The benchmark code is unlikely to benefit from improved bandwidth capabilities of additional memory levels. It suffers however from increased latency.

We consider this a typical property of many HPC codes which are heavily tuned to be arithmetically intense and to exploit vectorization. We also consider cache optimization to be a typical characteristics of many HPC codes.

Pinning and hyperthreading. Pinning is essential on many codes to achieve reasonable performance. However, we have not been able to confirm that pinning is important for our code. No data are presented here, as no statistically pinning impact could be observed:

Observation 7. Runtimes with and without pinning can hardly be distinguished.

As our code is extremely cache efficient, data resides in the cache close to the core. If the system should decide to migrate a running task, the cache content has to be moved, too. However, a code with such extremely localised data access usually does not run into traditional cache conflicts and false sharing.

Hyperthreading and oversubscription are a second powerful technique with deep memory hierarchies (Fig. 1) and on systems where floating point units are shared between physical threads: Data requests by a thread which cannot be served by a near cache trigger cache transfers. Meanwhile, the system swaps this thread with another compute thread until the data eventually has arrived. This is similar to the streaming compute paradigm in CUDA. While one thread uses the floating point capabilities, other threads can fetch/prepare all data for the subsequent AVX usage and queue to continue once the first thread “releases” the vector units. This complements the streaming paradigm, as it steps in whenever one thread cannot utilize the vector registers efficiently alone, i.e. does not stream data through the AVX components.

Both techniques do not yield performance improvements in our case on Skylake or Broadwell (Table 3). They decrease the performance. This holds for all problem sizes.

Observation 8. Our code’s performance suffers from hyperthreading and thread oversubscription.

Table 3: Runtime changes on two processors for a typical simulation ($p = 7$ on a 27^3 initial grid with $\Delta\ell$ additional levels of refinement) if we use hyperthreading (2:1) or assign two threads to each logical core (4:1). All runtimes are normalised to a run without any hyperthreading, i.e. using one thread (T) per physical core (C).

T:C	$\Delta\ell = 0$	$\Delta\ell = 1$	$\Delta\ell = 2$
2:1	0.75	0.67	0.80
4:1	0.77	0.71	0.70

The result is not a surprise taking into account that the code relies heavily on data access localization and tasks with reasonably small memory footprint which have high arithmetic intensity. Within one task, the code streams data through the AVX components. Continuing with a subsequent task becomes expensive if this task’s data does not reside in a near cache. As a result, task switches are per construction expensive: They interrupt the AVX usage pattern by the current thread, while also the kick off of a new tasks very likely induces further cache misses.

Frequency and energy efficiency analysis. AVX operations have high memory demands, while they might in turn induce a frequency reduction if the chip exceeds its energy/temperature thresholds. Our results (Table 4) validate that the reduction in time-to-solution compensates for these two effects: With AVX, the executable delivers the results faster at lower energy footprint. This effect is the stronger the higher the polynomial order, i.e. the higher the arithmetic intensity of the heavy compute tasks. We stick to the vectorised code base from hereon.

Observation 9. Vectorization is advantageous in terms of total energy footprint.

We have not been able to observe any significant impact of the task character homogenization on the AVX impact. One might guess that intermixing computationally heavy with cheap tasks implies that not all cores run AVX at the same time, and the node thus does not throttle the speed as significantly. This is a hypothesis we have not been able to confirm.

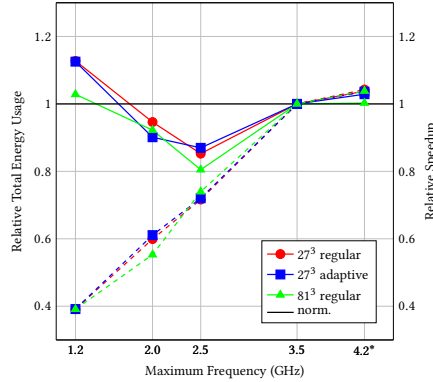
We continue with experiments on our Skylake testbed and manually modify the frequency of the chip. Frequency alterations affect all standard components’ maximum speed, while intense AVX usage still might reduce the frequency. Our data tracks the time-to-solution and the energy consumption per simulation run (Fig. 4).

Observation 10. Running a chip at maximum frequency is best in terms of time-to-solution. If energy per simulation however is the optimality condition, a significant reduction of the frequency is advantageous.

Our results are in line with reports on the best-case efficiency for Linpack if the total energy consumption has to be minimised [6]. Together with the memory bandwidth measurements, they however clarify that a frequency alteration does not change the character of our fundamental challenge: The more cores issue requests, the more our code suffers from latency effects. The deeper the cache hierarchy, the more severe these latency effects become.

Table 4: Energy consumption on Broadwell for a typical run with a regular and a dynamic grid. The total energy is given as well as the energy spent on the memory.

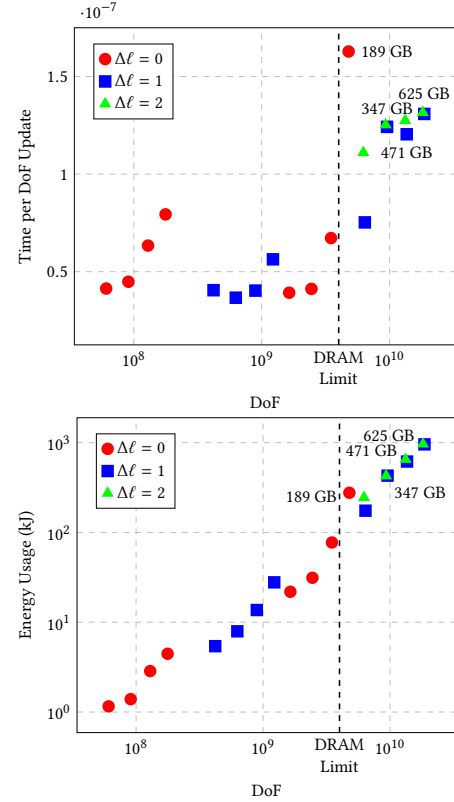
	Regular						Dyn. Adaptive					
	Scalar			AVX2			Scalar			AVX2		
	$p = 3$	$p = 5$	$p = 7$	$p = 3$	$p = 5$	$p = 7$	$p = 3$	$p = 5$	$p = 7$	$p = 3$	$p = 5$	$p = 7$
Total Energy (kJ)	3.52	10.7	31.8	2.61	5.87	19.1	85.1	106	227	51.3	77.4	198
Energy DRAM (kJ)	0.978	2.15	5.31	0.903	1.62	3.79	11.1	19.5	38.5	19.3	17.4	41.5

**Figure 4: Energy and time-to-solution results for various CPU frequencies on the Skylake machine without Optane memory for $p = 6$ with and without dynamically adaptive refinement. We normalize results against the default frequency configuration of 3.5 GHz without TurboBoost. 4.2 GHz* refers to a configuration with a base clock of 3.5 GHz with up to 4.2 GHz TurboBoost. Solid line represent energy and dashed lines the time-to-solution. These measurements do not use Optane.**

Optane memory. Finally, we scale up our problem size such that it does not fit into the main memory of the Skylake system anymore. We use IMDT, with configuration when DDR memory was configured as cache, and Intel Optane as main memory. While this improves the scalability compared to Fig. 2 due to standard weak scaling arguments, we do not study scaling further. Instead, we focus on memory usage.

For the benchmarking, we study $p \in \{6, 7, 8, 9\}$ and start from two regular grids: 27^3 and 81^3 . These regular grids are denoted by $\Delta\ell = 0$, as we add 0 levels of dynamic adaptivity. Starting from this setup, we also conduct experiments with up to two additional resolution levels of dynamica meshes. All data is plotted against the real degrees of freedom with up to 625 GByte total memory usage on a single node (Fig. 5).

We observe a rather homogeneous runtime cost per degree of freedom both for regular and dynamic grids. This cost is almost independent of the adaptivity which is due to the task-based nature of our code. We track one cost peak for a regular grid where we transition from runs without Optane-needs into runs where Optane is used. While we cannot explain this peak, we observe that the runtime cost with Optane remains under control:

**Figure 5: Skylake experiments for various problem sizes. Setups left of the dotted line use no Optane as everything fits into the DRAM, so we switch it off. Top: Time per degree of freedom update. Bottom: Total energy usage.**

Observation 11. As our code is cache-oblivious, we can exploit IMDT efficiently. We pay a penalty of a factor of 2–3.

As the dynamically adaptive mesh intermixes memory-intense and arithmetically demanding tasks stronger, Optane’s runtime penalty is more significant for the regular grid setups. While our code shows an almost linear correlation of total energy cost to degree of freedom count, the actual cost per degree of freedom update remains bounded for runs without Optane (less than $4 \cdot 10^9$ DoFs) and with Optane.

Observation 12. The energy demands per unknown update and the runtime per degree of freedom update are independent of the

problem size but determined by the number of memory levels used.

While the cache optimization of an HPC code ensures that Optane's latency penalty throttles the code performance infrequently, IMDT's prefetching logic relying on pattern analysis and real-time tuning struggles to predict the memory needs of a solver based upon dynamic adaptive meshes and, hence, dynamic task graphs. The IMDT can't know about our beyond-memory memory requests. We consider this to be a pattern of many important HPC codes: Data access exhibits stream access behaviour close to the compute core. On a higher level, codes however rely on flexible, dynamic tasks and thus do not fit to hardware tailored to stream access. Nevertheless, a runtime penalty of 2.5 seems to be very reasonable compared to Optane's specification.

Observation 13. As the energy demands for Optane are independent of the CPU clocking, the downclocking of the main memory has less impact on the energy-per-solution ratio than on a system without Optane.

5 SUMMARY AND CONCLUSION

Computer memory designers operate in a magic triangle of size, bandwidth and latency. Under given energy and cost constraints, not all three of these characteristics can be improved. While caches optimize for bandwidth and latency, the new Intel Optane memory optimizes for size and bandwidth. Our benchmarks clarify that existing cache optimization techniques—notably a high data access localization—pay off for this new memory level, too. They help to soothe the impact of massively increased latency.

In return, we observe that the idea to trade latency for bandwidth faces problems for our HPC codes: High throughput can be exploited via massive threading, but the context switches are too expensive. At the same time, the classic energy-saving concept to reduce the processor frequency loses some of its impact. Here, new algorithmic ideas have to be developed, and novel architecture concepts might be advantageous.

In the case of ExaHype, multi-task parallelism mixing tasks of different compute characteristics allowed us to mask Optane latency with DDR4 cache. The resulting performance decline is only 2x, which seem tolerable given an order of magnitude growth of attainable problem size. We propose four directions of future research:

- Future task systems should internally be sensitive to the compute character of the tasks. They have to mix compute-intense jobs with memory-intense jobs to avoid that a whole node waits for slow deep memory. This naturally can be mapped onto job priorities and mechanisms ensuring that not too many jobs of one priority are launched. At the moment, we observe that TBB even lacks a mature support for priorities.
- Prefetching of data should be part of any scheduler, as latency becomes a dominating factor. Modern schedulers should be able to look ahead, and it is easy to ask scientific developers to equip their tasks with a prefetching routine.
- With the reduced impact of frequency reductions, novel mechanisms to reduce the energy consumption are required. In the

context of memory and very dynamic codes, we propose to equip nodes with the opportunity to switch off threads or reduce the frequency of particular threads; to balance concurrency and bandwidth requirements with latency constraints.

- The other way round, it would be advantageous to obtain more control over the added deep memory. Our results suggest that a frequency reduction there lead to improved energy efficiency.

Machines equipped with Optane provide ample memory fit for even the largest simulations. Optane thus is an appealing alternative to classic “fat nodes”; also in terms of procurement cost. Once the exascale era makes the total power budget of computers grow to tens of megawatts, it is an option to trade, to some degree, the DRAM for an energy-modest extra layer of memory. This paper's results support the viability of this approach. More quantitative performance and power consumption models however are required.

ACKNOWLEDGMENTS

The authors appreciate support received from the European Union Horizon 2020 research and innovation programme under grant agreement No 671698 (ExaHyPE). This work made use of the facilities of the Hamilton HPC Service of Durham University. Particular thanks are due to Henk Slim for supporting us with Hamilton. Thanks are due to all members of the ExaHyPE consortium who made this research possible; notably M. Bader and J.-M. Gallard for integrating aggressively optimised compute kernels into ExaHyPE, and M. Bader, K. Duru, A.-A. Gabriel and L. Rannabauer for realising a seismic benchmark on top of ExaHyPE. The authors are particular thankful to Leonhard Rannabauer for the support on running the seismic benchmarks. All underlying software is open source [1].

REFERENCES

- [1] M. Bader, M. Dumbser, A.A. Gabriel, H. Igel, L. Rezzolla, and T. Weinzierl. ExaHyPE—an Exascale Hyperbolic PDE solver Engine, 2014–2019. <http://www.exahype.eu>.
- [2] K. Boyandin. Guest post: Intel optane and in-memory databases, obtained 29/08/2018. <https://blog.selectel.com/guest-post-intel-optane-and-in-memory-databases>.
- [3] D. Charrier, B. Hazelwood, and T. Weinzierl. Enclave tasking for discontinuous galerkin methods on dynamically adaptive meshes. 2018. arXiv:1806.07984 (submitted).
- [4] D. Charrier and T. Weinzierl. Stop talking to me—a communication-avoiding ADER-DG realisation. 2018. arXiv:1801.08682 (submitted).
- [5] M. Dumbser and M. Käser. An arbitrary high-order discontinuous Galerkin method for elastic waves on unstructured meshes - II. The three-dimensional isotropic case. *Geophysical Journal International*, 167(1):319–336, 2006.
- [6] D. Gessler. *Road to exascale: improving scheduling performances and reducing energy consumption with the help of end-users*. PhD thesis, Grenoble Alpes, 2016.
- [7] RSC Group. RSC launches HPC-targeted hyper-converged solution based on proven RSC Tornado architecture utilizing the newest Intel® SSD DC P4511 and Intel® Optane® SSD P4800X M.2 with IMDT, obtained 09/09/2018. <http://www.rscgroup.ru/en/news/347-rsc-launches-hpc-targeted-hyper-converged-solution-based-proven-rsc-tornado-architecture>.
- [8] A. Heinecke, A. Breuer, S. Rettenberger, M. Bader, A.-A. Gabriel, C. Pelties, A. Bode, W. Barth, X.-K. Liao, K. Vaidyanathan, M. Smelyanskiy, and P. Dubey. Petascale High Order Dynamic Rupture Earthquake Simulations on Heterogeneous Supercomputers. pages 3–14. IEEE, November 2014.
- [9] M. Kowarschik and C. Weiß. An Overview of Cache Optimization Techniques and Cache-Aware Numerical Algorithms. In U. Meyer, P. Sanders, and J. F. Sibeyn, editors, *Algorithms for Memory Hierarchies 2002*, pages 213–232, 2003.
- [10] Microway. Detailed Specifications of the Intel Xeon E5-2600v4 Broadwell-EP Processors.
- [11] J. Reinders. *Intel Threading Building Blocks*. O'Reilly, 2007.
- [12] J. Treibig, G. Hager, and G. Wellein. LIKWID: A Lightweight Performance-Oriented Tool Suite for x86 Multicore Environments. In *Proceedings of the 2010*

- 39th International Conference on Parallel Processing Workshops, ICPPW '10*, pages 207–216. IEEE Computer Society, 2010.
- [13] T. Weinzierl. The Peano software—parallel, automaton-based, dynamically adaptive grid traversals. *ACM Transactions on Mathematical Software*, 2018. (submitted; arXiv:1506.04496).
 - [14] T. Weinzierl and M. Mehl. Peano—A Traversal and Storage Scheme for Octree-Like Adaptive Cartesian Multiscale Grids. *SIAM J. Sci. Comput.*, 33(5):2732–2760, 2011.
 - [15] WikiChip. Xeon Gold 6154—Intel, obtained 09/09/2018. https://en.wikichip.org/wiki/intel/xeon_gold/6154.